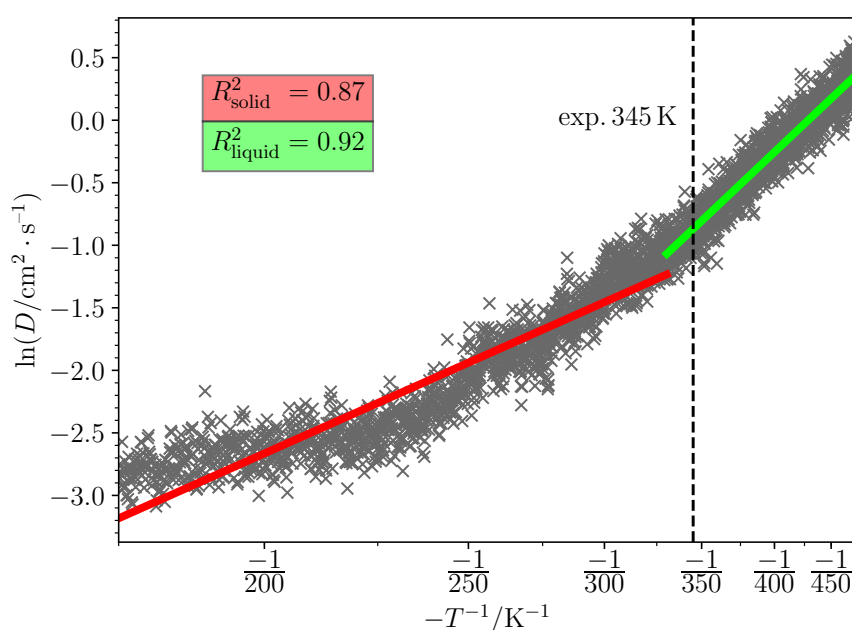


# Supplementary Materials: PREDICTING MELTING POINTS OF BIOFRIENDLY CHOLINE-BASED IONIC LIQUIDS WITH MOLECULAR DYNAMICS

Karl Karu , Fred Elhi, Kaija Põhako-Esko  and Vladislav Ivaništšev \*

## 1 Additional figures

2 Below are all figures of diffusion coefficient temperature ( $D - T$ ) dependences of the systems  
3 that were used to determine the melting point of the corresponding ionic liquids. Red, green, and  
4 dotted lines indicate respectively the fitted solid phase region, the fitted liquid phase region, and the  
5 experimental melting point.



**Figure S1.** The diffusion coefficient ( $D$ ) dependence on temperature ( $T$ ) during annealing simulation of Choline Acetate. The solid phase was packed at  $1.0 \text{ kg/dm}^3$  density with potential wells in CsCl lattice with 3:3:2 vector ratio.

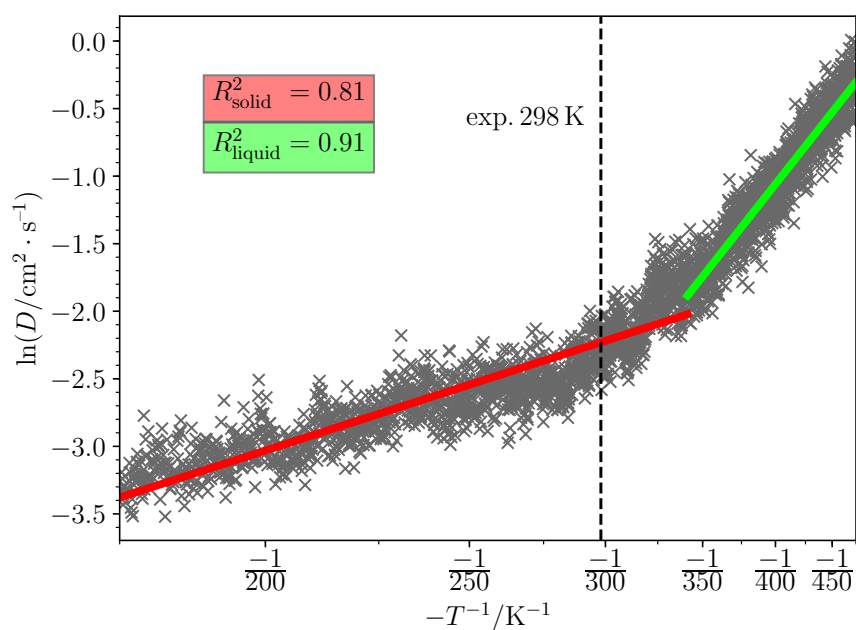


**Figure S2.** The diffusion coefficient ( $D$ ) dependence on temperature ( $T$ ) during annealing simulation of Choline Acesulfamate. The solid phase was packed at  $1.6 \text{ kg/dm}^3$  density with potential wells in NaCl lattice with 4:3:2 vector ratio.

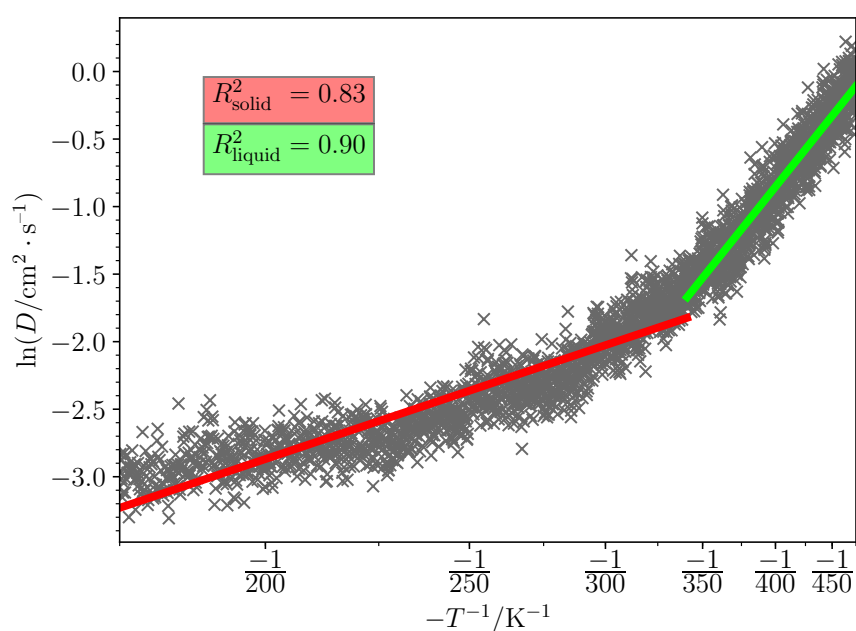


**Figure S3.** The diffusion coefficient ( $D$ ) dependence on temperature ( $T$ ) during annealing simulation of Choline Acetylsalicylate. The solid phase was packed at  $1.2 \text{ kg/dm}^3$  density with potential wells in NaCl lattice with 3:3:2 vector ratio.

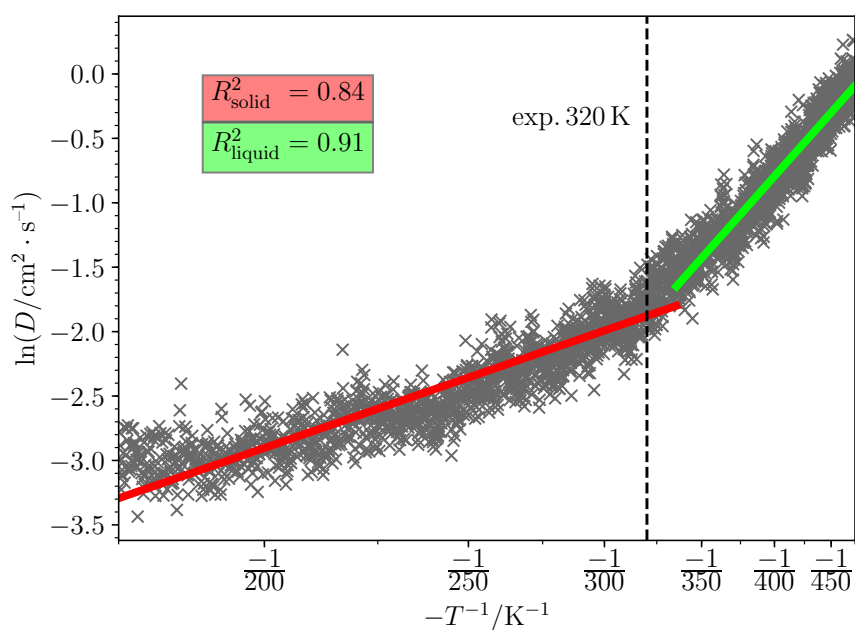


**Figure S4.** The diffusion coefficient ( $D$ ) dependence on temperature ( $T$ ) during annealing simulation of Choline Benzoate. The solid phase was packed at  $1.2 \text{ kg/dm}^3$  density with potential wells in CsCl lattice with 3:3:3 vector ratio.

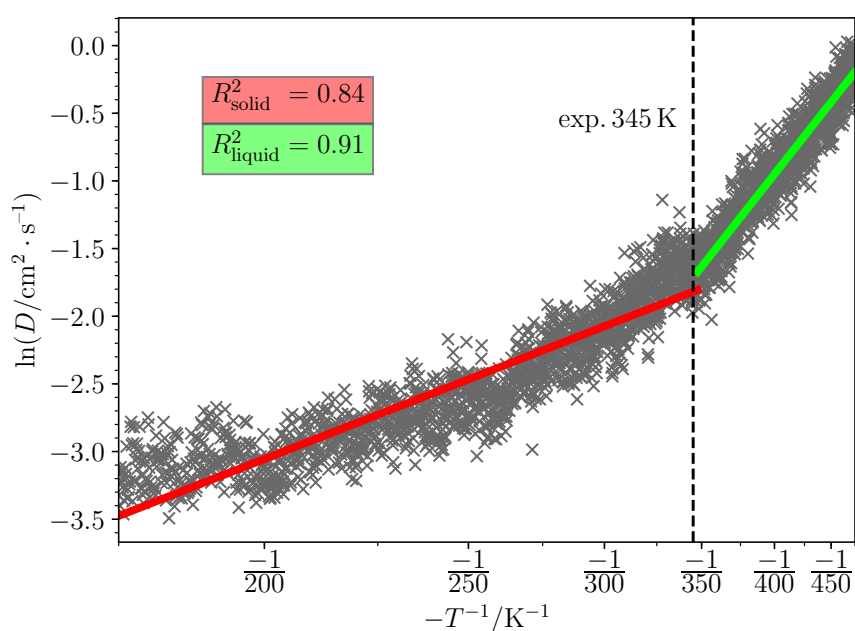


**Figure S5.** The diffusion coefficient ( $D$ ) dependence on temperature ( $T$ ) during annealing simulation of Choline Citrate. The solid phase was packed at  $1.2 \text{ kg/dm}^3$  density with potential wells in CsCl lattice with 3:2:2 vector ratio.

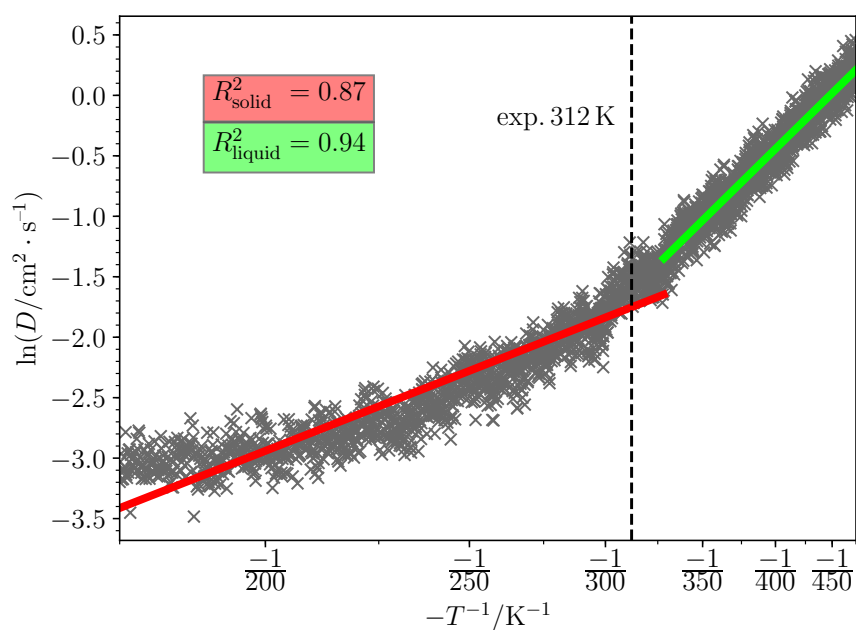


**Figure S6.** The diffusion coefficient ( $D$ ) dependence on temperature ( $T$ ) during annealing simulation of Choline Glutarate. The solid phase was packed at  $1.4 \text{ kg/dm}^3$  density with potential wells in NaCl lattice with 3:3:3 vector ratio.

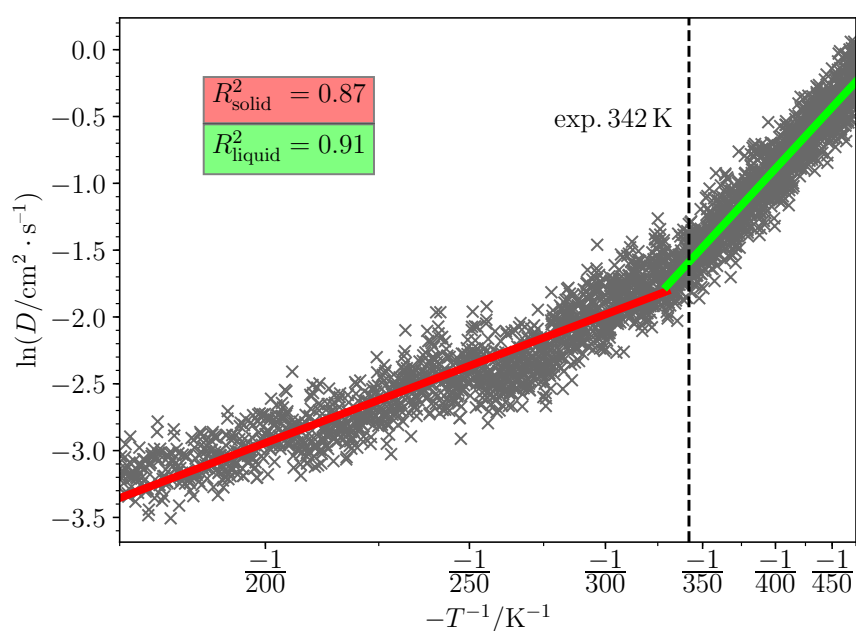


**Figure S7.** The diffusion coefficient ( $D$ ) dependence on temperature ( $T$ ) during annealing simulation of Choline Ibuprofenate. The solid phase was packed at  $1.2 \text{ kg/dm}^3$  density with potential wells in CsCl lattice with 4:3:2 vector ratio.

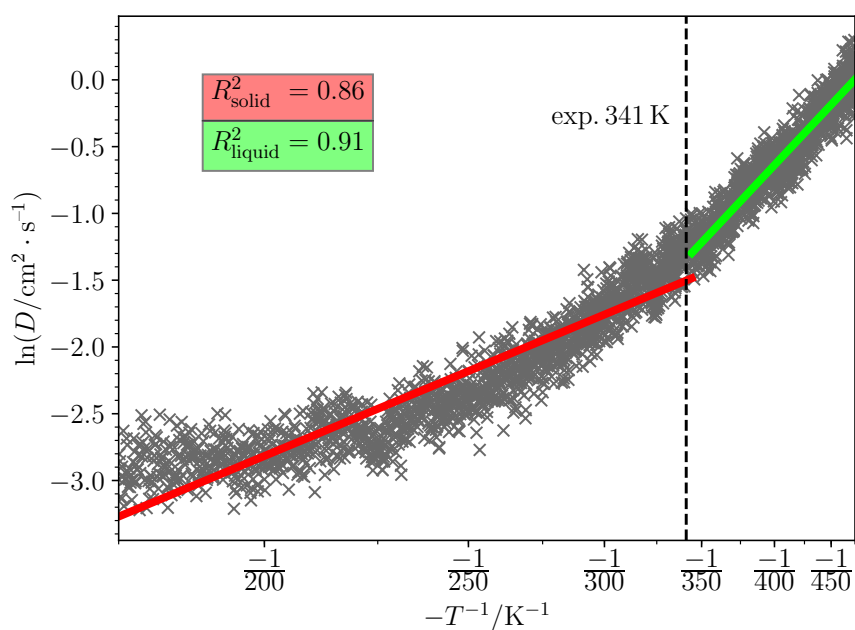


**Figure S8.** The diffusion coefficient ( $D$ ) dependence on temperature ( $T$ ) during annealing simulation of Choline Isobutanoate. The solid phase was packed at  $1.0 \text{ kg/dm}^3$  density with potential wells in CsCl lattice with 3:3:2 vector ratio.

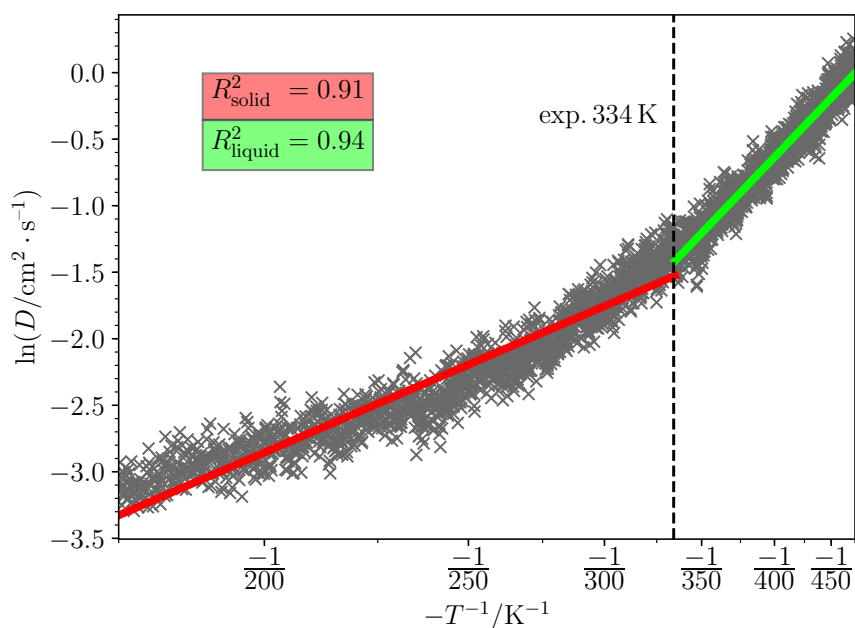


**Figure S9.** The diffusion coefficient ( $D$ ) dependence on temperature ( $T$ ) during annealing simulation of Choline Isovalerate. The solid phase was packed at  $1.2 \text{ kg/dm}^3$  density with potential wells in CsCl lattice with 4:3:2 vector ratio.

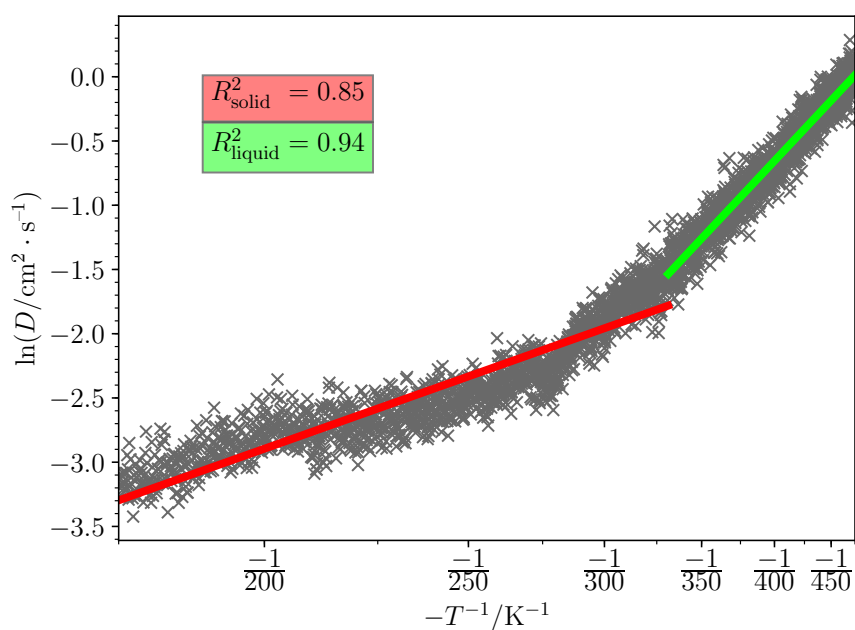


**Figure S10.** The diffusion coefficient ( $D$ ) dependence on temperature ( $T$ ) during annealing simulation of Choline Lactate. The solid phase was packed at  $1.4 \text{ kg/dm}^3$  density with potential wells in CsCl lattice with 3:3:3 vector ratio. Dotted line in this case marks the experimental glass phase transition temperature.

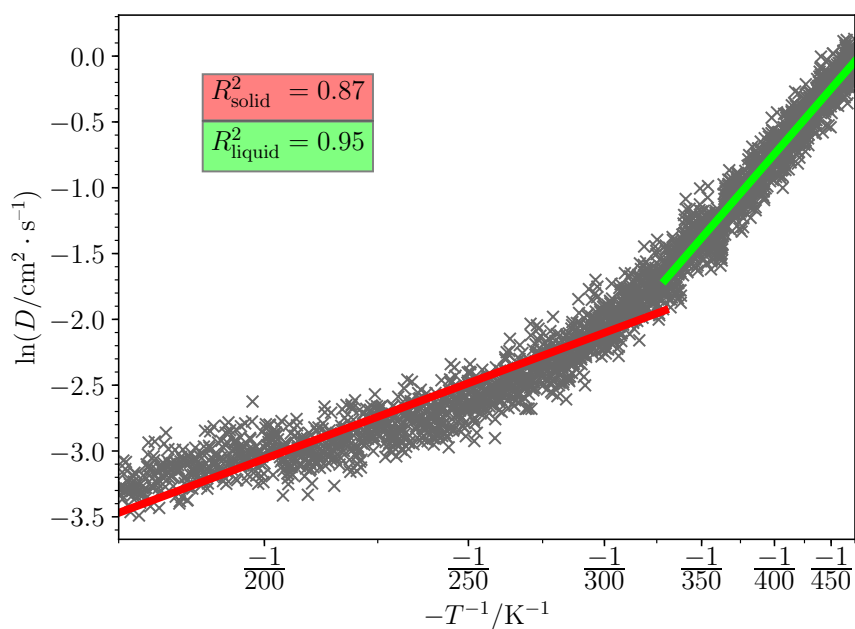


**Figure S11.** The diffusion coefficient ( $D$ ) dependence on temperature ( $T$ ) during annealing simulation of Choline Malonate. The solid phase was packed at  $1.4 \text{ kg/dm}^3$  density with potential wells in NaCl lattice with 4:3:2 vector ratio.

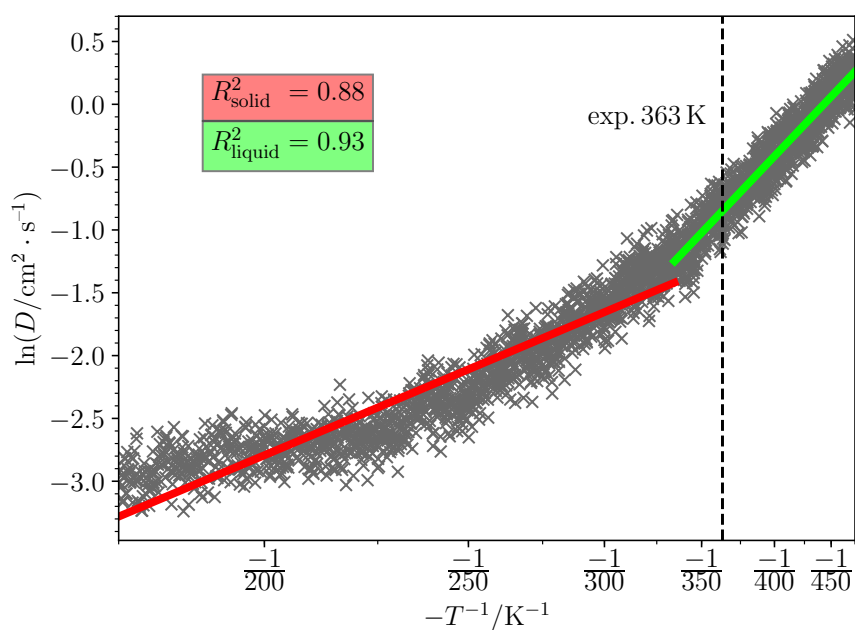


**Figure S12.** The diffusion coefficient ( $D$ ) dependence on temperature ( $T$ ) during annealing simulation of Choline 2-Methylbutanoate. The solid phase was packed at  $1.2 \text{ kg/dm}^3$  density with potential wells in CsCl lattice with 3:2:2 vector ratio.

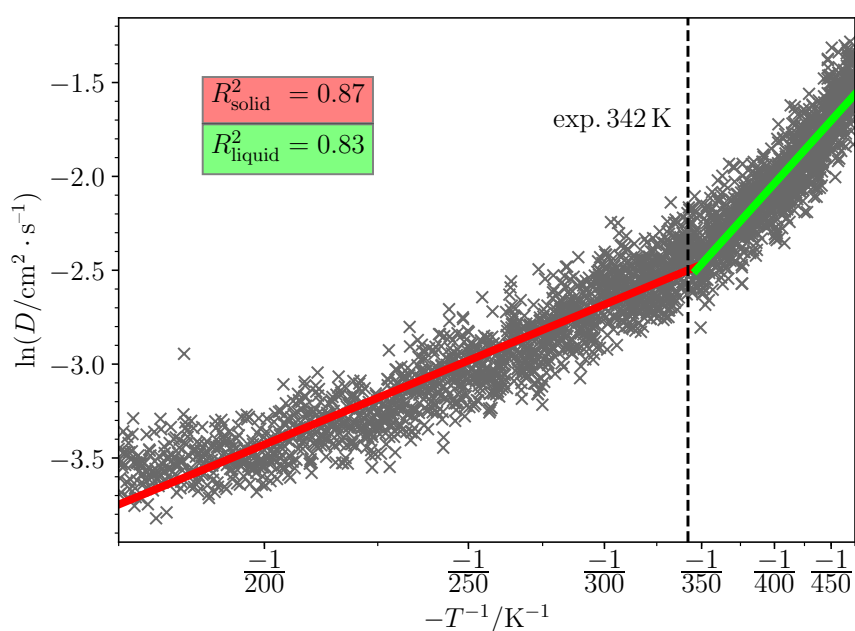


**Figure S13.** The diffusion coefficient ( $D$ ) dependence on temperature ( $T$ ) during annealing simulation of Choline Saccharinate. The solid phase was packed at  $1.6 \text{ kg/dm}^3$  density with potential wells in NaCl lattice with 3:2:2 vector ratio.

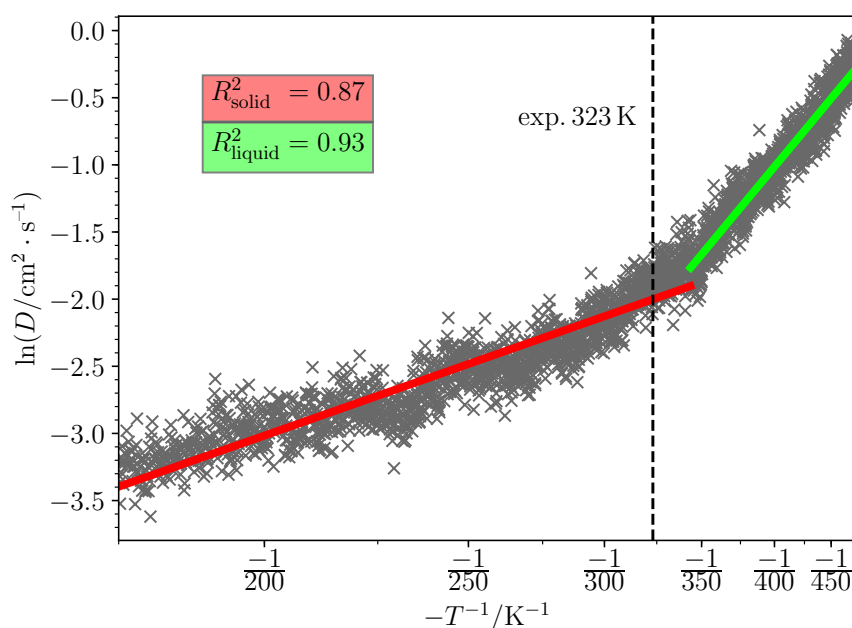


**Figure S14.** The diffusion coefficient ( $D$ ) dependence on temperature ( $T$ ) during annealing simulation of Choline Salicylate. The solid phase was packed at  $1.2 \text{ kg/dm}^3$  density with potential wells in CsCl lattice with 4:3:2 vector ratio.

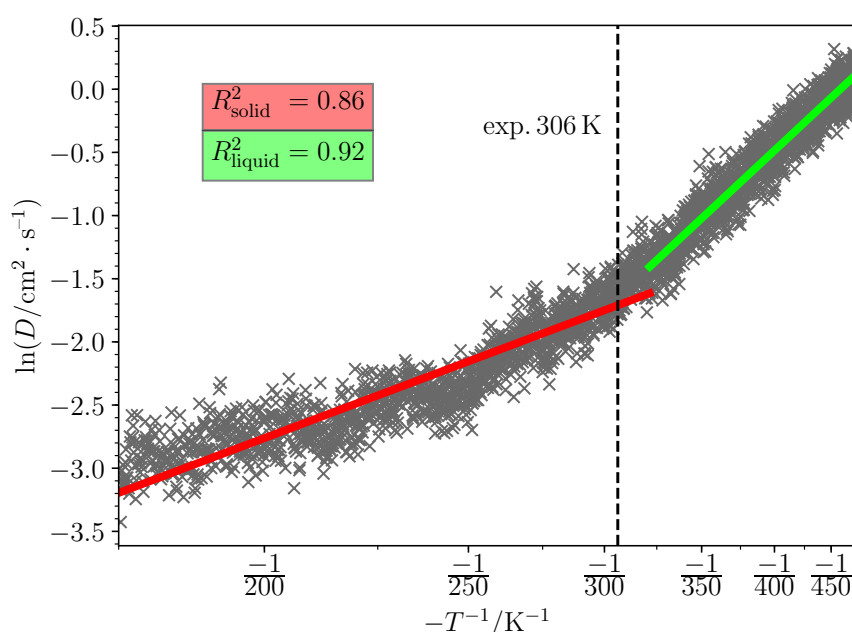


**Figure S15.** The diffusion coefficient ( $D$ ) dependence on temperature ( $T$ ) during annealing simulation of Choline TFSI. The solid phase was packed at  $1.6 \text{ kg/dm}^3$  density with potential wells in CsCl lattice with 4:3:2 vector ratio.

#### 6 Extrapolated melting point prediction

- 7 Melting point predictions obtained from simulations with different temperature rates were used  
 8 to extrapolated towards temperature rate  $0 \text{ K} \cdot \text{ns}^{-1}$ . The extrapolated melting point prediction is,  
 9 thus, the regression line intercept in Figure 5. The obtained results are in the table below. Only one



experimental value for each IL is chosen – the value used for root-mean-square-error calculation. Root-mean-square-error for regular predictions ( $10 \text{ K} \cdot \text{ns}^{-1}$ ) was 18–24K and root-mean-square-error for extrapolated predictions was 19–23K depending on the choice of experimental reference. With the exclusion of choline 2-methylbutanoate the error of extrapolated results is 12–18K compared to that of 17–22K.

**Table S1.** Experimental, predicted and extrapolated melting points ( $T_M$ ).

| Cation: choline<br>Anion | Experimental<br>$T_M$ (K)                   | Predicted<br>$T_M$ (K) | Extrapolated<br>$T_M$ (K) |
|--------------------------|---|------------------------|---------------------------|
| Acesulfamate             | 298 [1]                                     | 341                    | 325                       |
| Acetate                  | 353 [2], 324 [3], 345 [4], 354 <sup>a</sup> | 330                    | 340                       |
| Benzoate                 | 320 [3]                                     | 335                    | 332                       |
| Citrate                  | 345 [5], 376 [6], 378 <sup>a</sup>          | 348                    | 347                       |
| Glutarate                | 312 [7]                                     | 328                    | 323                       |
| Ibuprofenate             | 342 [8]                                     | 330                    | 340                       |
| Isobutanoate             | 308 [2], 341 <sup>a</sup>                   | 344                    | 337                       |
| Isovalerate              | 334 <sup>a</sup>                            | 335                    | 334                       |
| 2-Methylbutanoate        | 363 <sup>a</sup>                            | 335                    | 313                       |
| Saccharinate             | 342 [1]                                     | 347                    | 346                       |
| Salicylate               | 323 [9]                                     | 343                    | 339                       |
| TFSI                     | 306 [10]                                    | 321                    | 325                       |

<sup>a</sup> – measured in this work

## References

- Nockemann, P.; Thijs, B.; Driesen, K.; Janssen, C.R.; Van Hecke, K.; Van Meervelt, L.; Kossmann, S.; Kirchner, B.; Binnemans, K. Choline Saccharinate and Choline Acesulfamate: Ionic Liquids with Low Toxicities. *J. Phys. Chem. B* **2007**, *111*, 5254–5263. doi:10.1021/jp068446a.
- Petkovic, M.; Ferguson, J.L.; Gunaratne, H.N.; Ferreira, R.; Leitao, M.C.; Seddon, K.R.; Rebelo, L.P.N.; Pereira, C.S. Novel biocompatible cholinium-based ionic liquids - toxicity and biodegradability. *Green Chem.* **2010**, *12*, 643–649. doi:10.1039/B922247B.
- Fukaya, Y.; Iizuka, Y.; Sekikawa, K.; Ohno, H. Bio ionic liquids: room temperature ionic liquids composed wholly of biomaterials. *Green Chem.* **2007**, *9*, 1155–1157. doi:10.1039/b706571j.
- Muhammad, N.; Hossain, M.I.; Man, Z.; El-Harbawi, M.; Bustam, M.A.; Noaman, Y.A.; Mohamed Alitheen, N.B.; Ng, M.K.; Hefter, G.; Yin, C.Y. Synthesis and Physical Properties of Choline Carboxylate Ionic Liquids. *J. Chem. Eng. Data* **2012**, *57*, 2191–2196. doi:10.1021/jc300086w.
- Li, Z.; Liu, X.; Pei, Y.; Wang, J.; He, M. Design of environmentally friendly ionic liquid aqueous two-phase systems for the efficient and high activity extraction of proteins. *Green Chem.* **2012**, *14*, 2941–2950. doi:10.1039/c2gc35890e.
- Mourao, T.; Tome, L.C.; Florindo, C.; Rebelo, L.P.N.; Marrucho, I.M. Understanding the Role of Cholinium Carboxylate Ionic Liquids in PEG-Based Aqueous Biphasic Systems. *ACS Sustain. Chem. Eng.* **2014**, *2*, 2426–2434. doi:10.1021/sc500444w.
- Rengstl, D.; Fischer, V.; Kunz, W. Low-melting mixtures based on choline ionic liquids. *Phys. Chem. Chem. Phys.* **2014**, *16*, 22815–22822. doi:10.1039/C4CP02860K.
- Diogo, H.P.; Moura Ramos, J.J. Study of the thermal behavior of choline ibuprofenate using differential scanning calorimetry and hot-stage microscopy. *J. Mol. Struct.* **2014**, *1078*, 174–180. doi:10.1016/j.molstruc.2014.02.031.
- Wolf, J.; Aboody, R. Choline salicylate: a new and more rapidly absorbed drug for salicylate therapy. *Int. Record. Med.* **1960**, *173*, 234–241.
- Villanueva, M.; Parajo, J.; Sanchez, P.B.; Garcia, J.; Salgado, J. Liquid range temperature of ionic liquids as potential working fluids for absorption heat pumps. *J. Chem. Thermodyn.* **2015**, *91*, 127–135. doi:10.1016/j.jct.2015.07.034.